Water diffusion measurements in cement paste, mortar and concrete using a fast NMR based technique

Marc Fleury, Thibaud Chevalier, Guillaume Berthe, W. Dridi, M. Adadji

WATER DIFFUSION MEASUREMENTS IN CEMENT PASTE, MORTAR AND CONCRETE USING A FAST NMR BASED TECHNIQUE.

M. Fleury [(1)], T. Chevalier [(1)], G. Berthe [(1)], W. Dridi [(2)], M. Adadji [(3)]

[(1)] *IFP Energies nouvelles, 1 et 4 avenue de Bois-Préau, F- 92852, Rueil-Malmaison, France*
[(2)] Den-Service d'Etude du Comportement des Radionucléides (SECR), CEA, Université de Paris-Saclay, F-91191, France
[(3)] *ORANO, Direction Maîtrise d'Ouvrage Démantèlement et Déchet, 125 avenue de Paris, F-92320, Chatillon, France*

Abstract

With a NMR based fast diffusion measurement technique we performed a comprehensive experimental program on 30 samples to measure the pore diffusion coefficient in two series of cement pastes, mortar and concrete made with an ordinary Portland cement (CEM I) and a composite cement (CEM V). In addition, measurements were also possible in the presence of fibers and their effect could be evaluated. The principle is to monitor a deuterium-water exchange in a well-defined cylindrical geometry while the NMR technique allows the measurement of ^1H concentration inside the sample as a function of time, while ignoring ^1H outside the sample. Using well known analytical formulations, the diffusion curve can be fitted to obtain the pore diffusion coefficient of the material.

The results are first presented in terms of the measured pore diffusion coefficient at 30°C characterizing the porous network independently of porosity. For CEM I based materials, the measured values are D_p=7.6±1.4x10^{-12} m^2/s for pastes, 40±20x10^{-12} m^2/s for pastes with fibers, 9.5±0.6x10^{-12} m^2/s for mortars, 4.4±0.2x10^{-12} m^2/s for concretes and 28±7x10^{-12} m^2/s for concretes with fibers. For CEM V based materials, the measured values are D_p=1.1±0.4x10^{-12} m^2/s for pastes, 9.3±2.7x10^{-12} m^2/s for pastes with fibers, 0.8±0.1x10^{-12} m^2/s for mortars, 5.9±2.2x10^{-12} m^2/s for concretes and 5.3±0.8x10^{-12} m^2/s for concretes with fibers. In all cases, the fibers produce an increase of D_p together with a sample dependent result within a set of 3. When expressed in terms of effective diffusion by taking into account the porosity that can be exchanged by D_2O estimated during the diffusion experiments, the results were found in agreement with a few existing values measured with HTO through diffusion techniques (D_p=2.1±0.4x10^{-12} m^2/s for the CEMI paste, 1.1±0.06x10^{-12} m^2/s for the CEMI mortar, 0.12±0.02x10^{-12} m^2/s for the CEMV concrete with fibers).

1 Introduction

Concretes are used as diffusion barriers for the disposal of low and intermediate level radio-active waste. Diffusion properties are therefore of primary importance and such material are essentially qualified by a measurement of water diffusivity in a fully saturated state after a long hydration period (6 months) in order to reach a quasi-stable structure. Because concrete is a mixture of mainly cement, sand and sorted aggregates in which secondary but crucial products in minor quantities are added like silica fume, any changes in the formulation or in the quality of the constituents (e.g. mineralogy of the aggregates) requires a new validation. This can be a very lengthy and costly process as the measurement of water diffusion with standard tritium through diffusion (HTO) technique can be very time consuming, of the order of 1 to 4 years depending on the concrete and sample size.

To generate a diffusion barrier, one strategy is to find a binder with the smallest intrinsic (pore) diffusion coefficient and then decrease porosity as much as possible to obtain the smallest effective diffusion coefficient by the addition of sand and aggregates. Adding aggregates also have the important property of improving considerably the compressive strength. However, the potential negative impact is to create interfacial transition zones (ITZ) [1,2], thin regions around aggregates in which a different microstructure exist together with a local larger porosity. Minimizing ITZ effects is still a challenge, requiring numerous diffusion experiments. ITZ effects may also play an important role when adding fibers to improve further the mechanical properties. The choice of the type of cement is also important, with potential effects on the ITZ. For ordinary Portland cement, ITZ has been suspected to play an important role while other cement like CEM V in which silica fume is added for example, have much lower porosities and consequently could minimize ITZ effects.

While the HTO through diffusion technique is well established, efforts have been made to speed up experiments or find alternate techniques [4]. For example, the in-diffusion technique in which a concentration profile is measured, the electro-migration technique to obtain the transport properties of ions accelerated in an electrical field, or simply formation factor measurements; however they are for the last two cases strongly model dependent and applicable to ions only. In the present study, concrete reinforced with metallic fibers were also of high interest, limiting further the possible range of alternate techniques. Considering now nuclear magnetic resonance (NMR), the well-known Pulsed Field Gradient NMR technique providing water self-diffusion coefficients without the need for tracer cannot be applied in some materials. In most cementitious materials and especially after complete hydration [3] the very short life time of the magnetization unfortunately prevails the use of this very reliable and fast technique. In this work, we use a method in which a water saturated sample is fully immersed in deuterium; as the exchange between water and deuterium is taking place, the water concentration inside the sample can be measured using simple NMR sequences as a function of time and analyzed to obtain a diffusion coefficient. It could be labeled inside-out diffusion. This technique was already used in cement 20 years ago [5] and curiously not developed further. In natural porous media and constrained by the same short magnetization life time, the same technique was re-developed and compared to HTO through diffusion [6]; it was then applied again on various cementitious materials [7] with different geometrical configurations, also taking advantage of the technological development of fully automated low field relaxometers and progress in data processing such as inverse Laplace transform.

Since various terminologies are present in literature such as effective, apparent or pore diffusion coefficients, it is important to clarify our notation especially when introducing a method not commonly used. As detailed in [4,6], since we measure a concentration inside the sample and not a tracer flux through the sample we directly obtain a pore diffusion coefficient. In a standard through diffusion experiment one obtain an effective diffusion coefficient when analyzing the steady state regime [4]. The so-called pore diffusion coefficient noted D_p is linked to the effective diffusion D_e by the relationship:

$$D_p = D_e / \phi \tag{1}$$

where Φ is the exchangeable porosity discussed later. Furthermore, ^2H interactions with cement should not be different from ^1H and therefore we obtain a true determination of D_p. In practice, the experiments are shorter when measuring D_p instead of D_e. D_p is an intrinsic property of the porous network contributing to diffusion and it may stay ideally the same when considering a cement paste and a mortar or concrete made with the same cement, ignoring ITZ effects. Hence D_e experiments like HTO through-diffusion will be typically 3 times longer as porosity is decreasing. Finally, if one would like to take adsorption effects into account, the coefficient measured in this work would then correspond to an apparent pore diffusion coefficient D_a defined as:

$$D_a = D_p (1 - \rho_S K_d) \tag{2}$$

where the adsorption process is described by a coefficient K_d (m^3/kg) and ρ_S is the dry density of the solid phase (kg/m^3).

In this work, we built a comprehensive 3-year measurement program to obtain pore diffusion coefficients for decreasing porosities starting from the cement paste, then the mortar and finally the concrete. In addition metallic fibers were added on the cement paste and the concrete to evaluate their effects. We first describe these materials. Next, we describe in some details the measurement methodology including uncertainty analysis in which we consider random effects of noise and heterogeneity. Finally, the results are described and grouped according to the type of cement.

2 Materials

Two types of cements were tested: (i) an ordinary Portland cement (CEM I) and (ii) a blended cement with silica fume (CEM V). Two types of fibers were also included both in the cement pastes and the concrete. Hence, for each cement type, 5 different materials were prepared: a cement paste

with and without fibers, a mortar, and a concrete with and without fibers. Testing 3 samples of each material resulted in a total of 30 experiments.

Cement pastes and mortars were prepared according to the standard fabrication procedure NF EN 196-1. The mixtures proportions are given in Table 1. Cylindrical samples (diameter = 7 cm, height = 11 cm) were cast and the molds were sealed during the first 24 h. After demolded, samples were kept in a saturated lime water incorporating sodium and potassium hydroxide for more than 6 months. Also during diffusion experiments and immersion into deuterium, deuterium was equilibrated with lime to maintain the pH around 11.5 and avoid chemical evolution or structural changes of the samples during the experiments. The first molded samples were made from a CEM I cement and they are denoted PI and PI-F for CEM I pastes without and with fibers respectively. The second ones were made from a CEM V cement and they are denoted PV and PV-F for CEM V pastes without and with fibers respectively. The mortars prepared either with CEMI or CEMV are denoted MI and MV.

Concretes with and without fibers were cast within a cylindrical mold (diameter = 11 cm, height = 22 cm). Some details of formulation are given in Table 2. After demolding, samples were stored in lime water under the same conditions as cement pastes and mortars. The NMR test samples were cored before measurements close to the centre cores. CT-scan performed prior to drilling indicates the presence of more air bubbles near the top of the cylinders. The porosity is therefore expected to fluctuate slightly, as will be seen below. It should be noted that metallic fibers used in PI-F and CI-F materials have a length of 35 mm and a diameter of 0.55 mm. The ones used in PV-F and CV-F materials have a length of 30 mm, a width of 1.6 mm and a thickness of 29 µm.

Table 1: mixture proportions for cement pastes (P) and mortars (M) for ordinary Portland (I) and blended (V) cement. The letter F indicates the presence of fibers. For example, PI-F is a paste made of cement CEMI and containing fibers.

	PI (kg/m^3)	PI-F (kg/m^3)	PV (kg/m^3)	PV-F (kg/m^3)	MI (kg/m^3)	MV (kg/m^3)
Cement	1397	1370	1338	1383	699	669
Sand					1310	1310
Water	559	548	535	553	279	267
Fibers		100		30		

Table 2: mixture proportions for concrete with and without fibers

	CEM I based concrete (CI) (kg/m^3)	CEM V based concrete (CV) (kg/m^3)
Cement	480	430
Sand	700	700
Gravel	600	900
Filler	200	60
Silica fume	50	20
Metallic fibers	100 (conventional)	30 (amorphous)
Superplasticizers	10	10
Water	200	170

3 Experimental methods

3.1 Principle

The method used in this work was partially developed earlier in the framework of the measurement of water diffusion in tight natural porous media (in particular caprocks [6]) and also validated in various cement based material [7] may contain metallic fibers for mechanical reinforcement, the material ultimately used in practice. We will only describe here the aspects necessary for understanding the technique and its advantages or limits when applied to cement based materials. The details of the measurements and in particular the detailed NMR aspects can be found elsewhere [7]. The two instruments used in this study are permanent magnet relaxometers from Oxford Instruments; for cements and mortars without fibers (sample of diameter of about 9 mm and length 12mm), the NMR

probe size was 18 mm and the proton Larmor frequency f_L was 23.7 MHz; for concretes and samples with fibers, the NMR probe size was 30 mm and f_L was 20.3 MHz.

The principle of the method is illustrated in Fig. 1; a sample initially saturated with water is immersed into deuterium, everything being contained in a NMR glass tube. For cementitious materials, it is important to keep a high pH and both water and deuterium were saturated with lime. As the result of the diffusion of ^1H outside and ^2H inside the porous sample, the ^1H concentration inside the sample will gradually decrease; using the NMR technique detailed in [7] and sensitive only to ^1H, we can distinguish the protons outside the sample from those inside using the strong relaxation contrast between them (1 vs. 3000 ms) and obtain in an easy and robust way the number of protons inside the sample as a function of time. In practice the recorded NMR signal was a Hahn echo at 0.13ms for concretes, and a free induction decay (FID) for cement pastes and mortars, both repeated such as not to polarize the long components (i.e. apply a repeat delay between scans of 100 ms without recording the first scan). The magnetization M used to calculate a proton concentration (see below) at a given diffusion time is the maximum of either the FID or Hahn signal. When 500 scans for example are accumulated, a single measurement takes about 5s.

As usual with NMR techniques, we measure a magnetization signal M proportional to the number of protons in the investigated volume which can then be calibrated with a known volume of water, taking into account the characteristics of the probe and various acquisition parameters such as the gain of amplifiers. The size of the sample is related to the NMR probe used and therefore on the equipment available in a given laboratory. Indeed, the sample size must be such that the filling factor is not too small, otherwise the signal to noise ratio may correspondingly be to small; for example, a 10 mm probe can accommodate cylindrical samples with a diameter of 9 to 5 mm and length of up to 10 mm, a 18 mm probe from 16 down to 10 mm and length of up to 18 mm. In this study, the cement paste and mortar samples were cylinders with a diameter of approximately10 mm and length around 15 mm, while concrete samples were cylinders with diameter of about 20 mm and length of about 20 mm. As experimental duration generally depends on the square of the smallest length-scale, the choice of these diameters and lengths were driven by compromise between representative elementary volume consideration and experimental durations, as will be discussed later.

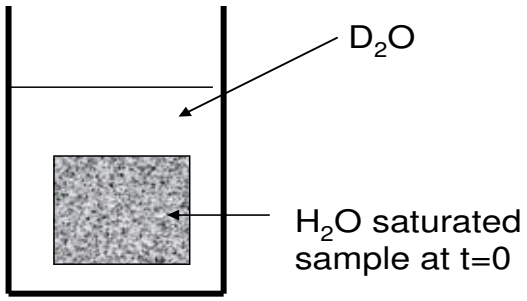

Fig. 1. Principle of the method. A sample initially saturated with water is placed in a NMR tube. Then, D_2O is poured onto the sample defining a zero time for diffusion. The ^1H concentration inside the sample is then measured as a function of time, as ^1H is diffusing out and ^2H into the sample. Both water and deuterium are saturated with lime.

An example of measurement is shown in Fig. 2. The concentration is defined as the magnetization M normalized by the initial magnetization at the diffusion time t_D=0 (start of the diffusion experiment when deuterium is poured onto the sample):

$$C = \frac{M(t_D)}{M(t_D = 0)} \tag{3}$$

The sealed glass tube is usually left in the NMR instrument regulated at a temperature of 30°C±0.1°C at the start of the diffusion experiment where a relatively fast variation of concentration is measured (corresponding at two weeks non-stop recordings).Then, the glass tube is carefully transferred in an oven also regulated at 30°C (another temperature can also be chosen). This explains the lack of data points from time to time (Fig. 2). When the asymptotic concentration is reached, measurements are only necessary every 10 or 20 days. In this example, a diffusion coefficient can be already fitted with

good accuracy taking data points up to t_D=2500 hours (104 days), the last data points are only useful for confirming the good stability of the measurements.

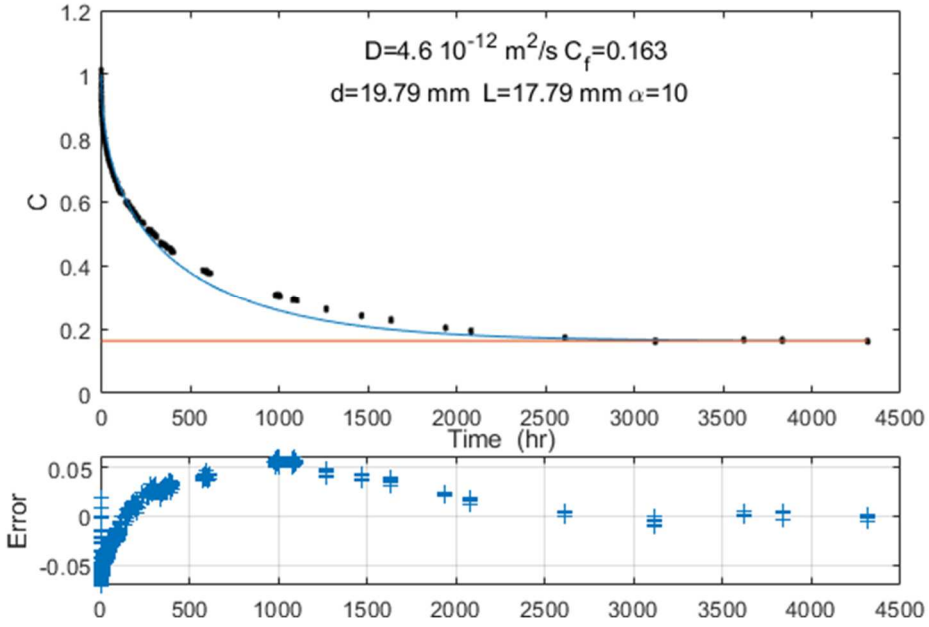

Fig. 2. Example of measurement of the ^{1}H concentration C as a function of time in a concrete sample of diameter 19.79 mm and length 17.79 mm (CI A). In the upper panel, black dots represent the measurements and the curve the fitted model yielding D_e=4.6 10^{-12} m^2/s and C_f=0.163. The horizontal line indicates the fitted asymptotic concentration C_f at infinite time. In the lower panel, the points represent the difference between the model and the measurement at each acquisition point.

3.2 Data analysis

To analyze the data, we used the well-known analytical formulations and methodologies detailed in Crank [8] and Carslaw & Jaeger [9]; the solution of a diffusion equation in a cylinder of length $L=2l$ and radius $r=d/2$ is the product of two terms, C_{ps} and C_{cyl}, respectively representing the diffusion in a plane sheet ("ps") and in an infinite cylinder ("cyl"), and are given by: (equations 4.37 and 5.33 in [8])

$$C^* = \frac{M(t_D) - M(t_D = \infty)}{M(t_D = 0) - M(t_D = \infty)} = C_{ps} C_{cyl} \tag{4}$$

$$C_{ps} = \sum_{n=1}^{\infty} \frac{2\alpha(1+\alpha)}{1+\alpha+\alpha^2 p_n^2} \exp\left(-D_p p_n^2 \frac{t_D}{l^2}\right) \tag{5}$$

$$C_{cyl} = \sum_{n=1}^{\infty} \frac{4\alpha(1+\alpha)}{4+4\alpha+\alpha^2 q_n^2} \exp\left(-D_p q_n^2 \frac{t_D}{r^2}\right) \tag{6}$$

where p_n are the non-zero positive roots of the equation $\tan p_n = -\alpha p_n$, q_n the non-zero positive roots of the equation $\alpha q_n J_0(q_n) + 2J_1(q_n) = 0$, α is the volumetric D_2O/H_2O ratio. These equations have been established for boundary conditions corresponding to our experimental situation: a cylinder immersed in D_2O such that the total volume H_2O + D_2O is constant. Hence the D_2O concentration at the cylinder surface is strictly not constant and this is taken into account by the factor α. The assumption is that the mixture D_2O/H_2O is well stirred outside the cylinder; this is a reasonable assumption since the diffusion coefficient of H_2O or D_2O outside the cylinder is several orders of magnitude larger compared to the ones inside the cylinder. Since α is always kept experimentally at a value close to 10 (the amount of D_2O is large compared to H_2O), this parameter has little influence and it was set to the value of 10 in the calculations.

The diffusion experiment also gives access to the exchangeable porosity, i.e. the porosity in which ^1H can be replaced by ^2H; indeed, if the entire pore volume V_p is exchangeable, the asymptotic ^1H concentration will be:

$$C_{eq} = \frac{V_p}{V_D + V_p} \approx \frac{V_p}{V_D} = \frac{1}{\alpha} \tag{7}$$

where V_D is the deuterium volume. In this case, ^1H concentration is the same inside and outside the sample. If the measured asymptotic concentration $C_f = M(t_D=\infty)/M(t_D=0)$ is different from C_{eq}, then the exchangeable porosity Φ_{ex} will be:

$$\Phi_{ex} = \Phi(1 - C_f - C_{eq}) \tag{8}$$

Since C_f is necessary for calculating C* but not always measured precisely, our fitting program based on Matlab not only optimizes the D_p coefficient in equation 5 and 6 but also $M(t_D=\infty)$ in equation 4. This will be further considered when discussing uncertainties. Note that deuterium in this method cannot be considered as a tracer because its concentration will finally be very large in the sample, of the order of $1-1/\alpha$ (~90%).

3.3 Robustness and uncertainties

We first estimated uncertainties due to random noise in a data set using Monte Carlo methods (Fig. 3). A decay curve was generated using equations 3 to 6 (D_e=1.0x10^{-11} m^2/s, asymptotic concentration of 0.1) mimicking the acquisition protocol (lack of data during certain periods) and then we added a random noise of significant amplitude. In addition, the numerical data set is such that the asymptotic concentration is not reached in order to consider a very unfavourable situation potentially producing more uncertainties. Our fitting procedure was then performed for 100 random noise realizations. The results indicate a relatively small standard deviation in the distribution of the fitted D_p values; we find D_p=0.97±0.02 10^{-11} m^2/s close to the input value of 1.0x10^{-11} m^2/s. The lack of data at long times in the asymptotic region generates a systematic small underestimation. Such results representative of the most unfavorable situations indicate that the measured diffusion coefficients are fairly robust relative to random noise.

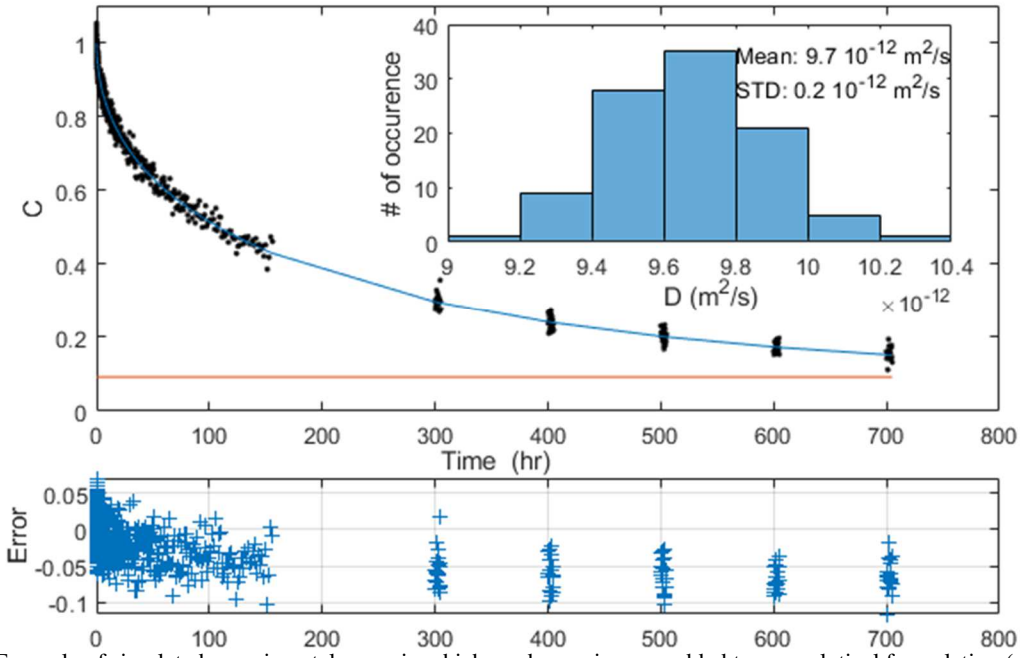

Fig. 3. Example of simulated experimental curve in which random noise was added to an analytical formulation (equations 3 to 6). The data set was also designed such as to reproduce the experimental protocol including a lack of data during certain periods. The inset shows the histogram of the fitted values for 100 random noise realizations.

Another source of uncertainties is linked to heterogeneity issues. As mentioned above, measurement on concrete samples cannot be performed on 10 mm cylindrical samples due the presence of non-porous aggregates of significant size (a few millimetres). At a scale of 20 mm, the tested concrete samples cannot be considered as truly homogeneous, whereas the analytical formulation assumes that diffusion can occur in the entire volume and not only in the cement phase. By way of illustration, this issue was considered using numerical simulations of the diffusion in a cylinder containing various non-porous regions located on the surface or inside. For this purpose, the COMSOL software was used and a numerical decay curve of ^{1}H concentration generated and then analysed using our fitting procedure (Fig. 4). In the situation considered, we observe only small deviations between the analytical model and the numerical simulations, indicating that heterogeneity problem has little impact. It strongly suggests that the deviation between the model and the data of the order of 5% with obviously weak random noise in the example of Fig. 2 may effectively be due to heterogeneity effects. Two main reasons can be invoked in favour of a weak sensitivity of the method to heterogeneity effects: (i) diffusion processes generally have a high smoothing capacity and (ii) the diffusion process analysed occurs in 3 dimensions further increasing the smoothing capacity. We will see later that 3 measurements performed on 3 different samples yielded very similar values, confirming that the choice of 20 mm size samples in diameter and length is appropriate.

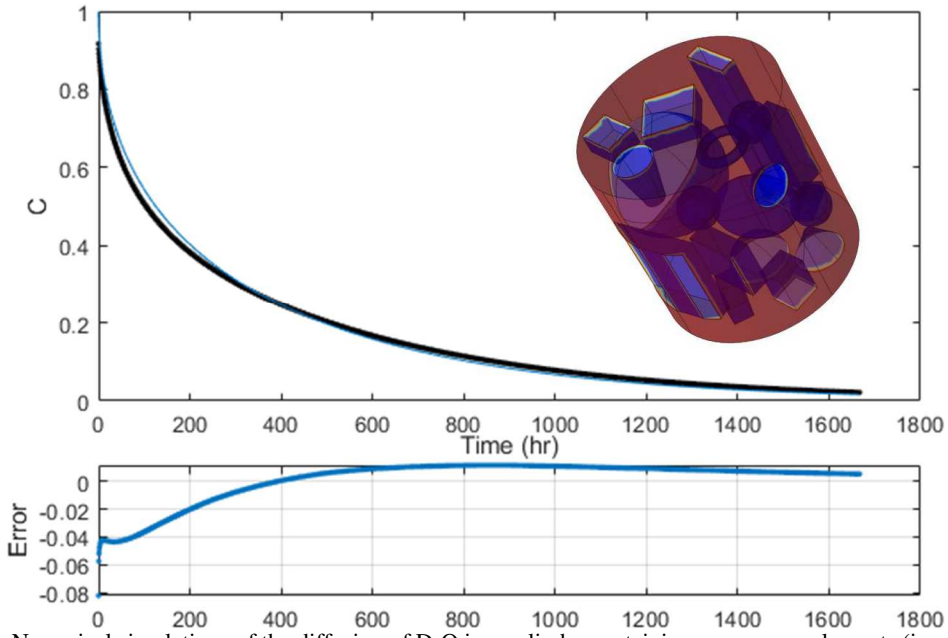

Fig. 4. Numerical simulations of the diffusion of D_2O in a cylinder containing non porous elements (inset) in which diffusion cannot occur (representing 25% of the total volume). The black thick curve represents the numerical simulations and the blue thin curve the analytical model.

3.4 Porosity

While porosity values are not used to interpret diffusion curves, they are necessary for practical calculation of diffusive fluxes. However when dealing with nanometric pore sizes the concept of porosity may become difficult because the meaning of bulk and surface water can be questioned. NMR techniques have the ability to distinguish different proton populations having different signatures [10]. Indeed, the NMR measurements are sensitive to protons in the solid crystalline structure, C-S-H interlayer, gel pore water and capillary water. Most NMR studies used this sensitivity to describe the structural changes during hydration up to typically 1 month, by analyzing for example the T_2 relaxation time distribution. Since we used samples with hydration period larger than 6 months, T_2 relaxation values expressing the existence of very small pores are consequently small (<1 ms) and the separation of the different proton populations becomes difficult and depends on the NMR instrument dead time of , a key characteristic in the present context. It should also be noted that most

NMR studies use the so-called white cement produced by selecting compounds low in paramagnetic species such as iron and manganese. Hence, the relaxation time contrast between "free water" and other species is less pronounced in normal cement.

Porosity can be estimated from usual Carr-Purcell-Meiboom-Gill (CPMG) measurements [10,11], a collection of magnetization data points following an initial pulse at time t=0 (Fig. 5). This CPMG curve was measured on a CEM V based concrete and is plotted using a logarithmic time scale to highlight the critical short time acquisition period. By fitting the data points with a sum of exponential decays $M(t) = \sum_i A_i \exp(t / T_{2i})$ (inverse Laplace transform) one obtains the T_2 distribution dominated by short relaxation times (~0.2 ms, inset of Fig. 5). The total number of protons in the system is given by M(t=0) and the dead time of this instrument is such that the first data point is obtained at t=0.13 ms. From literature, the separation between solid and liquid like protons may occur at a relaxation time of 0.1 ms [10,12,13]. Although numerically correct, the extrapolated value may overestimate free water volumes and a choice was made to calculate porosity (free water volume divided total geometric volume) using the first data point at t=0.13 ms.

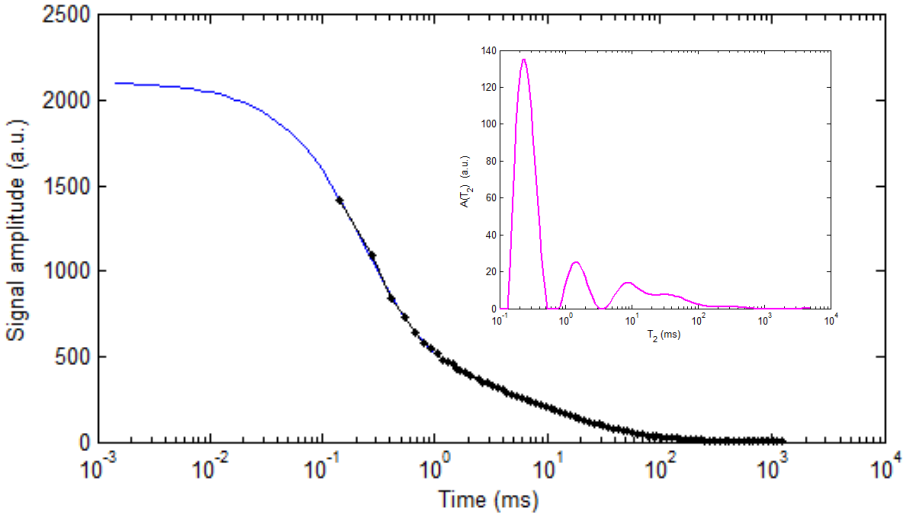

Fig. 5. Example of a CPMG measurement used to determine porosity. The blue line indicates the fitted multi-exponential model. The inset indicates the T_2 distribution inferred from the magnetization decay curve. After calibration with a known water volume, $M(t_1)$ using the first data point corresponds to a volume of 0.249 ml while the extrapolated value of M at t=0 gives 0.370 ml.

The above procedure was applied for all samples without fibers; in the presence of fibers, the impedance of the NMR probe is strongly modified and porosities can no more be deduced in a simple way by comparing signal amplitudes with a known water volume. Indeed, the NMR probe can be assimilated to a resonant LCR (inductance, capacitance and resistance) circuit those impedance is modified when introducing a very conductive material. To be valid and applicable, a measurement on a known water volume should also have similar impedance variation included but no robust method was found to mimic the strong probe perturbations. Hence, we assigned the same values of porosity for samples with fibers than without fibers. Porosities obtained by drying were found similar with and without fibers confirming that this approach is reasonable (see Table 3 and 4). The fibers have however no effect on the diffusion curves because a calibration of the signal is not necessary (equation 3); we verified also that the magnetization M is proportional to the water content in similar strong perturbations of the probe.

The exchangeable porosity is also of interest. For the example in Fig. 2, we have C_{eq}=0.052 and C_f=0.163. Hence only 89% of the porosity is exchangeable. The inferred values of Φ_{ex} from equation 8 obviously depend on the initial choice of the pore volume V_p. In the above example, even if we

double the value of V_p, we still obtain a non-negligible value of Φ_{ex}. Measured values for all samples are listed in Table 3.

4 Results

We report here all measured diffusion coefficients for CEM I and CEM V based materials. Data values are given in 3 tables (see appendix).

The measured pore diffusion coefficients for CEM I based materials are all plotted in Fig. 6. Without fibers, porosity values were measured by NMR as explained above. Since porosity could not be determined by NMR in the presence of fibers, the values used in the graph are the average of the paste and concrete respectively. As expected, the pore diffusion coefficient does not vary much between cement pastes and mortars despite a porosity decrease of about a factor of 2, and some fluctuations of porosity due to small local variations when preparing the plugs. Note that the duration of the experiments are all similar (400 to 700 hours, Table 3). For the concrete samples, there is a decrease of D_p from ~$8x10^{-12}$ m^2/s down to ~$4x10^{-12}$ m^2/s, meaning that the tortuosity of the pore network is slightly increased when adding agglomerates. With fibers, the observations are very different. For the cement pastes first, D_p increases significantly (from ~$8x10^{-12}$ m^2/s up to ~$40x10^{-12}$ m^2/s on average), and very large fluctuations between the 3 samples are observed (±$20x10^{-12}$ m^2/s). This is clearly an indication of preferential diffusion paths induced by the fibers that can vary from one sample to another depending on their location and length. Indeed, since the fibers initially used in the molds have a length of 35 mm, samples of 20 mm length and diameter are too short and may contain a variable number of fibers with different lengths and orientations. Hence the measured fluctuations indicate that the fibers have indeed a strong effect. For the concrete samples with fibers, fluctuations are also observed but attenuated due to the presence of agglomerates.

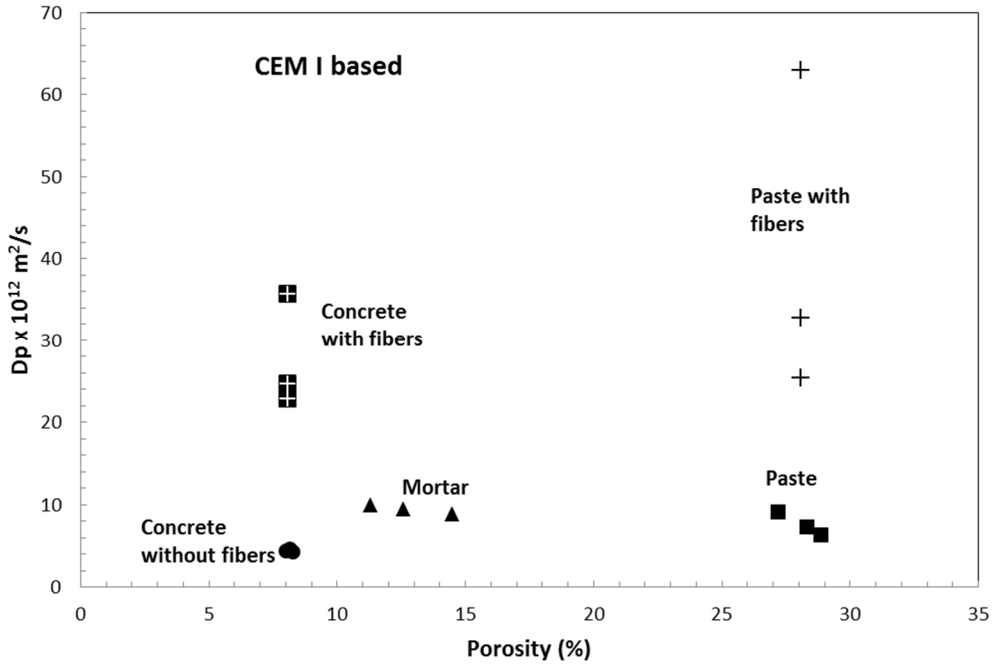

Fig. 6. Pore diffusion coefficients for CEM I based materials. Squares: pastes; crosses: paste with fibers; triangles: mortar; circles: concrete without fibers; squares including a cross: concrete with fibers.

Similar observations can be made concerning the results of CEM V based materials except for the concrete samples (Fig. 7). Without fibers, the pore diffusion coefficients are similar for the 3 pastes and mortars, whereas large fluctuations exists for concrete without fibers; on average, D_p increases from ~$1x10^{-12}$ m^2/s (pastes and mortars) up to ~$6x10^{-12}$ m^2/s (concretes). With fibers, there is a large increase of D_p for the pastes (on average from ~$1x10^{-12}$ m^2/s up to ~$9x10^{-12}$ m^2/s). As with CEM I

samples, a similar discussion can be made about the positions and lengths of the fibers, although they are thin and flat fibers of length 30 mm and not cylinders. For concrete with fibers, fluctuations of D_p are also observed, contained inside the range of D_p values without fibers.

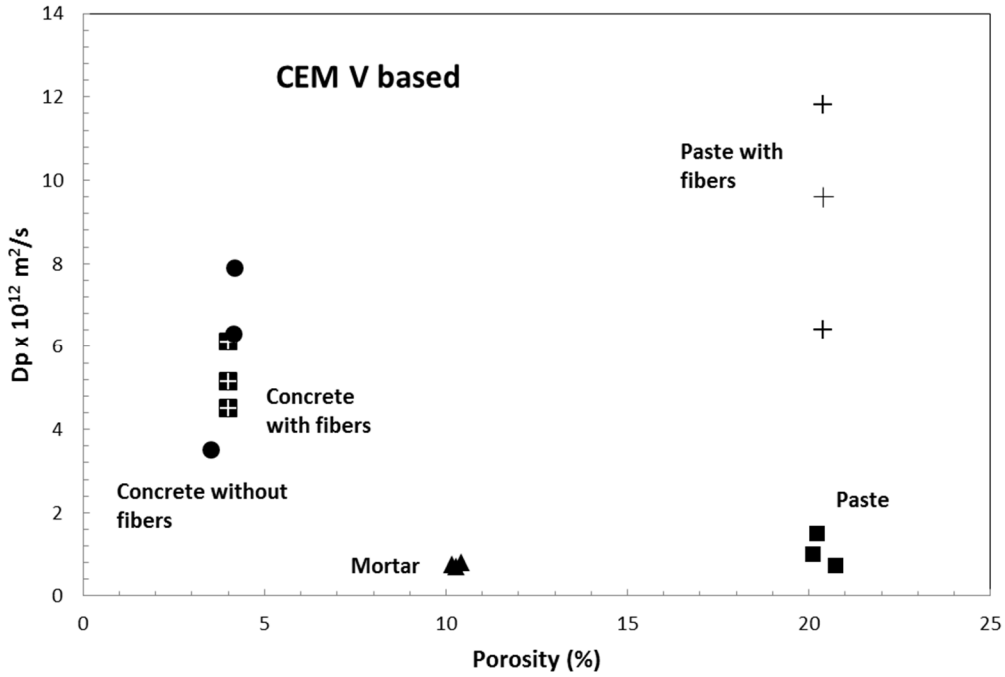

Fig. 7. Pore diffusion coefficients for CEM V based materials. Squares: pastes; crosses: paste with fibers; triangles: mortar; circles: concrete without fibers; squares including a cross: concrete with fibers.

5 Summary and conclusion

The diffusive transport properties of the different materials studied can be summarized by plotting the effective diffusion coefficient $D_e=\Phi_{ex} D_p$, product of the exchangeable porosity and the pore diffusion coefficient D_p (Fig. 8). The exchangeable porosity is deduced from the measurement of the asymptotic ^1H concentration at the end of the experiment. In the graph, we took the average value of the 3 measurements for each group. In this representation, D_e of mortar is decreasing compared to pastes solely due a decrease of porosity. For CEM I based materials, two D_e values were available from HTO through-diffusion techniques and performed on samples with the same formulation [14]; we observe a good agreement with our results for the paste and the mortar (Fig. 8 and Table 5).

The CEM V based materials have in general a much lower D_e than CEM I based materials due primarily to a lower D_p. Whereas the effect of the fibers is to increase considerably D_p as discussed above, it is balanced for the case of the concrete made with CEM V by a much lower exchangeable porosity; indeed, we observe that only 60% of the estimated porosity is exchangeablein the presence of fibers, whereas all the porosity is exchangeable without fibers. Hence, D_e tends to decrease slightly. We also obtain a good agreement (Fig. 8 and Table 5) with HTO through-diffusion measurements performed on concrete with fibers (ORANO, unpublished results). However, these comparisons depend on the choice of porosity values.

At this stage, we are not able to provide deeper insight about the detailed diffusion mechanisms occurring in these samples and we can only speculate. In the CEM I concrete case, the fibers may obviously accumulate ITZ effects strongly affecting diffusion properties. Furthermore, when D_p values vary significantly within a group of 3 samples, ITZ effects can be suspected because the diffusion measurements have a small intrinsic error (at most ±5%). Hence the final result depends on the particular configuration of a given sample (e.g. agglomerates or fibers locations). For the CEM I concrete, we obtain a very small standard deviation within the 3 samples, $D_p=4.4\pm0.2\text{x}10^{-12}$ m^2/s,

whereas for the CEM V concrete, it is much larger, D_p=5.9±2.2x10^{-12} m^2/s. But when adding fibers to the CEM V concrete, it is reduced again D_p=5.3±0.8x10^{-12} m^2/s suggesting a beneficial effect of fibers for lowering diffusion properties.

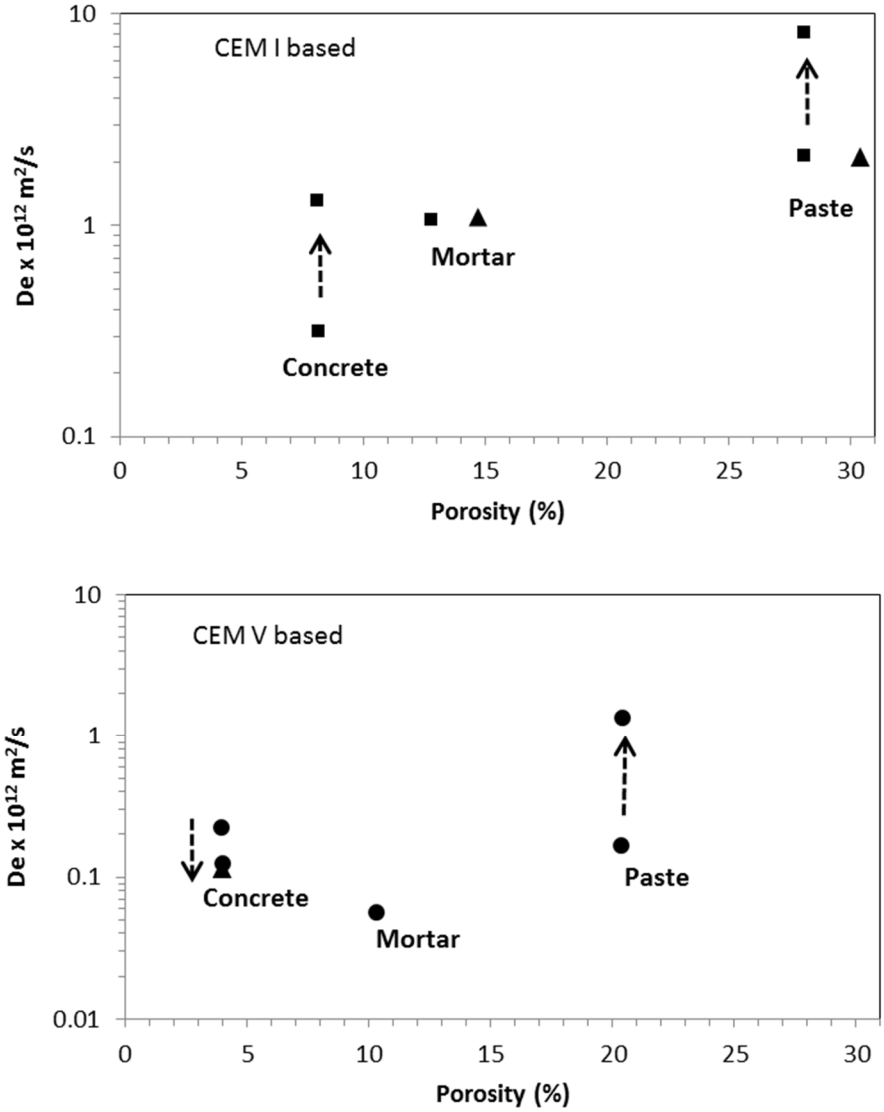

Fig. 8. Average effective diffusion coefficients for all types of materials studied based either on CEMI or CEMV. The dashed arrow indicates the inclusion of fibers into the material. The triangles indicate 3 available De values measured by HTO through diffusion techniques on samples made with the same formulation.

Acknowledgments

We thank Cedric Boher (ORANO TEMIS – Concrete Unit) for providing data on concrete and useful comments on the draft manuscript. We also thank ORANO and CEA for funding this research.

6 Appendix

The results are all summarized in Tables 3 to 5. The effective diffusion coefficient D_e is the product of D_p and the estimated exchangeable porosity Φ_{ex} according to equation 1. The issue of the appropriate porosity value is however quite important. For example, the porosity Φ_{drying} obtained by drying the sample at 105°C until a stable mass (±1%) is reached is always larger or much larger than Φ_{NMR}. Following Larbi et al. [14] and Gallé et al. [15], the drying temperature of 105°C may induced structural changes explaining these differences. Porosities obtained by Larbi et al. on cement pastes at a drying temperature of 60°C are close to our NMR values and we took the NMR values for converting pore to effective diffusion coefficients. The apparent density obtained after drying is also a useful indicator of possible anomalies inside a group of 3 samples; for example, mortar C (CEM I based material) has a much lower value of d_{app} than the two other samples, possibly due to the presence of bubbles in this particular sample; otherwise d_{app} is relatively uniform for all other groups, in particular in the presence of fibers; the fluctuations of the measured D_p values for these samples cannot be due to a difference in the numbers of fibers within each sample. The indicated duration of the experiment is a minimum necessary for reaching the asymptotic concentration value C_f; in many cases, data points were acquired for a longer period of time as in Fig. 2 to obtain a more accurate value of C_f. The exchangeable porosity Φ_{ex} is also indicated as a fraction of the estimated porosity Φ_{NMR}.

Table 3. Porosity and diffusion coefficients for 3 samples (A to C or D) of CEM I based materials: paste (P), mortar (M) and concrete (C). The presence of fibers is indicated by the letter F.

	d_{app} (g/cm^3)	D_p x10^{12} (m^2/s)	Φ_{drying}	Φ_{NMR}	Φ_{ex} (% Φ_{NMR})	D_e x10^{12} (m^2/s)	Duration (hrs)
PI A	2.03	6.3	35.6	28.9	29.2 (101)	1.8	700
PI B	2.04	7.3	34.5	28.3	27.8 (98)	2.0	700
PI C	2.03	9.1	35.6	27.2	27.3 (100)	2.5	700
PI-F A	2.05	32.7	32.3	28.1	20.4 (72)	6.7	500
PI-F B	2.08	25.3	33.0	28.1	21.0 (75)	5.3	600
PI-F C	2.04	62.9	33.7	28.1	19.2 (68)	12.1	400
MI A	2.30	8.9	17.3	14.5	13.0 (90)	1.2	400
MI C	1.94	10.0	15.4	11.3	9.9 (87)	1.0	400
MI D	2.26	9.5	18.2	12.6	10.9 (87)	1.0	400
CI A	2.32	4.6	17.7	8.2	7.2 (89)	0.3	2500
CI B	2.26	4.2	20.4	8.3	7.5 (90)	0.3	2500
CI C	2.29	4.4	20.2	8.0	7.0 (87)	0.3	2500
CI-F A	2.32	22.8	17.6	8.1	4.7 (58)	1.1	500
CI-F B	2.33	35.7	18.5	8.1	4.5 (56)	1.6	300
CI-F C	2.35	24.6	19.2	8.1	5.0 (62)	1.2	600

Table 4. Porosity and diffusion coefficients for 3 samples (A to C or D) of CEM V based materials: paste (P), mortar (M) and concrete (C). The presence of fibers is indicated by the letter F.

	d_{app} (g/cm^3)	D_p x10^{12} (m^2/s)	Φ_{drying}	Φ_{NMR}	Φ_{ex} (% Φ_{NMR})	D_e x10^{12} (m^2/s)	Duration (hrs)
PV B	1.82	1.0	40.3	20.1	15.9 (79)	0.16	3000
PV C	1.96	0.7	44.8	20.7	16.1 (78)	0.12	3000
PV D	1.88	1.5	41.0	20.2	14.8 (73)	0.22	3000
PV-F B	2.11	6.4	56.4	20.4	13.3 (65)	0.85	1600
PV-F C	2.17	9.6	44.3	20.4	16.1 (79)	1.15	1100
PV-F D	2.14	11.8	59.8	20.4	14.8 (73)	1.25	600
MV A	2.28	0.8	20.5	10.2	7.3 (72)	0.06	1800
MV C	2.24	0.7	21.6	10.3	7.7 (75)	0.05	1200
MV D	2.30	0.8	21.3	10.4	7.7 (74)	0.06	800
CV A	2.37	7.9	13.4	4.2	3.9 (92)	0.31	1500
CV B	2.36	6.3	13.6	4.1	4.0 (98)	0.26	1500
CV C	2.37	3.5	13.3	3.5	3.4 (98)	0.12	2000
CV-F B	2.35	6.1	15.5	4.0	2.4 (61)	0.15	2000
CV-F C	2.36	4.5	14.1	4.0	2.4 (60)	0.11	2500
CV-F D	2.35	5.2	13.8	4.0	2.4 (60)	0.12	3000

Table 5. Average diffusion coefficient and fluctuations calculated from the standard deviation of the 3 measurements. Some HTO tracer results performed on samples with the same formulation are also indicated. For the CEM I and CEM V based materials, the identical D_e values and uncertainties are coincidental.

	D_p x 10^{12} (m^2/s)	D_e x 10^{12} (m^2/s)
CEM I based material		
Paste (PI) HTO tracer [14]	7.6 ±1.4	2.1 ±0.4 2.1 ±0.4
Paste with fibers (PI-F)	40 ±20	8 ±4
Mortar (MI) HTO tracer [14]	9.5 ±0.6	1.1 ±0.06 1.1 ±0.06
Concrete (CI)	4.4 ±0.2	0.32 ±0.015
Concrete with fibers (CI-F)	28 ± 7	1.3 ±0.3
CEM V based material		
Paste (PV)	1.1 ±0.4	0.17 ± 0.06
Paste with fibers (PV-F)	9.3 ±2.7	1.36 ±0.4
Mortar (MV)	0.8 ±0.1	0.06 ±0.004
Concrete (CV)	5.9 ±2.2	0.22 ±0.084
Concrete with fibers (CV-F) HTO tracer (unpublished)	5.3 ±0.8	0.13 ±0.02 0.12 ±0.02

7 References

[1] J.P. Ollivier, J.C. Maso, B. Bourdette, Interfacial transition zone in concrete, Advanced Cement Based Materials 2 (1) (1995) 30–38. https://doi.org/10.1016/1065-7355(95)90037-3.

[2] K.L. Scrivener, A.K. Crumbie, P. Laugesen, The Interfacial Transition Zone (ITZ) Between Cement Paste and Aggregate in Concrete, Interface Science 12 (4) (2004) 411–421. https://doi.org/10.1023/B:INTS.0000042339.92990.4c.

[3] N. Nestle, P. Galvosas, J. Kärger, Liquid-phase self-diffusion in hydrating cement pastes — results from NMR studies and perspectives for further research, Cement and Concrete Research 37 (3) (2007) 398–413. https://doi.org/10.1016/j.cemconres.2006.02.004.

[4] R.A. Patel, Q.T. Phung, S.C. Seetharam, J. Perko, D. Jacques, N. Maes, G. de Schutter, G. Ye, K. van Breugel, Diffusivity of saturated ordinary Portland cement-based materials: A critical review of experimental and analytical modelling approaches, Cement and Concrete Research 90 (2016) 52–72. https://doi.org/10.1016/j.cemconres.2016.09.015.

[5] C. Choi, J. Peternelj, M.M. Pintar, A method for measuring the diffusivity of a liquid into a porous matrix, The Journal of Chemical Physics 109 (5) (1998) 1860–1862. https://doi.org/10.1063/1.476761.

[6] P. Berne, P. Bachaud, M. Fleury, Diffusion Properties of Carbonated Caprocks from the Paris Basin, Oil & Gas Science and Technology – Revue de l'Institut Français du Pétrole 65 (3) (2009) 473–484. https://doi.org/10.2516/ogst/2009072.

[7] M. Fleury, G. Berthe, T. Chevalier, Diffusion of water in industrial cement and concrete, Magnetic Resonance Imaging (2018). https://doi.org/10.1016/j.mri.2018.09.010.

[8] J. Crank, The mathematics of diffusion, 2nd ed., Clarendon Press, Oxford, 1976.

[9] H.S. Carslaw, J.C. Jaeger, Conduction of heat in solids, Oxford Science Publications, 1959.

[10] A. Valori, P.J. McDonald, K.L. Scrivener, The morphology of C–S–H: Lessons from 1H nuclear magnetic resonance relaxometry, Cement and Concrete Research 49 (2013) 65–81. https://doi.org/10.1016/j.cemconres.2013.03.011.

[11] S. Meiboom, D. Gill, Modified Spin-Echo Method for Measuring Nuclear Relaxation Times, Rev. Sci. Instrum. 29 (8) (1958) 688–691. https://doi.org/10.1063/1.1716296.

[12] R. Holly, E.J. Reardon, C.M. Hansson, H. Peemoeller, Proton Spin?: Spin Relaxation Study of the Effect of Temperature on White Cement Hydration, J American Ceramic Society 90 (2) (2007) 570–577. https://doi.org/10.1111/j.1551-2916.2006.01422.x.

[13] P.J. McDonald, V. Rodin, A. Valori, Characterisation of intra- and inter-C–S–H gel pore water in white cement based on an analysis of NMR signal amplitudes as a function of water content, Cement and Concrete Research 40 (12) (2010) 1656–1663. https://doi.org/10.1016/j.cemconres.2010.08.003.

[14] B. Larbi, W. Dridi, P. Dangla, P. Le Bescop, Link between microstructure and tritiated water diffusivity in mortars: Impact of aggregates, Cement and Concrete Research 82 (2016) 92–99. https://doi.org/10.1016/j.cemconres.2016.01.003.

[15] C. Gallé, Effect of drying on cement-based materials pore structure as identified by mercury intrusion porosimetry, Cement and Concrete Research 31 (10) (2001) 1467–1477. https://doi.org/10.1016/S0008-8846(01)00594-4.

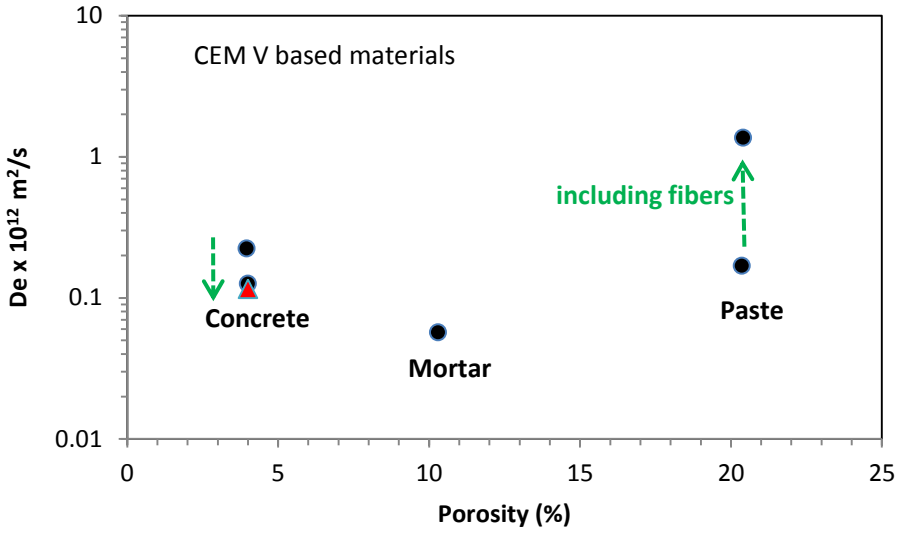
CEM V based materials
De x 10¹² m²/s
10
1
0.1
0.01
0
5
10
15
20
25
Porosity (%)
including fibers
Concrete
Mortar
Paste